PHYSICAL REVIEW D **96,** 076013 (2017)

Nontopological first-order vortices in a gauged $CP(2)$ model with a dielectric function

R. Casana,[1] M. L. Dias,[1] and E. da Hora[2]

[1]*Departamento de Física, Universidade Federal do Maranhão, 65080-805 São Luís, Maranhão, Brazil*
[2]*Coordenadoria Interdisciplinar de Ciência e Tecnologia, Universidade Federal do Maranhão, 65080-805 São Luís, Maranhão, Brazil*

(Received 30 August 2017; published 24 October 2017)

We consider nontopological first-order solitons arising from a gauged $CP(2)$ model in the presence of the Maxwell term multiplied by a nontrivial dielectric function. We implement the corresponding first-order scenario by minimizing the total energy, thus introducing the corresponding energy lower bound; such a construction is only possible due to a differential constraint that includes the dielectric function itself and the self-interacting potential defining the model. We saturate the aforementioned bound by focusing our attention on those solutions fulfilling a particular set of two coupled first-order differential equations. Next, in order to solve these equations, we choose the dielectric function explicitly, and also calculate the corresponding self-interacting potential. We impose appropriate boundary conditions that support nontopological solitons, from which we verify that the energy of final structures is proportional to the magnetic flux they engender: both quantities are not quantized, as expected. We depict the new numerical solutions, while commenting on the main properties they present.

DOI: 10.1103/PhysRevD.96.076013

I. INTRODUCTION

In the context of classical field theories, vortices are planar solutions coming from highly nonlinear gauged models [1]. In general, these solutions are calculated directly from the second-order Euler-Lagrange equations. However, under very special circumstances, they can also be obtained via a particular set of first-order differential equations which minimize the energy of the overall system [2]. In this case, the energy bound is expected to be proportional to the quantized magnetic flux the resulting first-order vortices engender. In particular, first-order vortices supporting quantized flux were first found within the canonical Maxwell-Higgs scenario, which gives rise to topological configurations only [3]. Later, both topological and nontopological vortices were also shown to exist in the Chern-Simons-Higgs electrodynamics [4].

Moreover, solitons inherent to nonstandard models were recently investigated, such as the ones arising from generalizations of the Abelian-Higgs systems [5], Lorentz-breaking scenarios [6], and gauged theories presenting unusual dynamics whose solutions were applied to study some interesting cosmological issues [7].

Therefore, it is certainly important to consider whether a gauged $CP(N-1)$ theory supports well-behaved first-order vortices, especially given that the $CP(N-1)$ model effectively mimics interesting properties of the Yang-Mills theories defined in four dimensions [8].

In a recent work [9], vortex solutions inherent to a gauged $CP(2)$ model in the presence of the Maxwell term were considered, and the corresponding solutions were obtained directly from the second-order Euler-Lagrange equations of motion. In addition, the existence of configurations satisfying a particular set of first-order differential equations was suggested. Then [10], a self-dual framework was developed that gave rise to the aforecited solutions, and explicitly introduced the corresponding first-order differential equations and the energy lower-bound. Moreover, it has been verified that the energy lower bound that the first-order solitons saturate is proportional to their magnetic flux, which is quantized according to the winding number of such configurations, as expected. Here, it is important to say that, due to the boundary conditions fulfilling the finite-energy requirement, such first-order solitons present topological properties.

In the context of noncanonical models, a rather natural issue is the study of the gauged $CP(2)$ theory endowed with the Maxwell term multiplied by a dielectric function depending on the scalar field only. The motivation regarding this nontrivial coupling comes from supersymmetric scenarios, in which such a nonstandard kinetic term is necessary to support a gauged model with a noncompact gauge group [11]. Also, field models with a dielectric function have additionally being used to study quarks and gluons via soliton bag theories [12].

It is known that, under special circumstances, a gauged theory provided with a nontrivial dielectric function can support both topological or nontopological solitons. In this sense, the aim of the present manuscript is to investigate the way such a noncanonical $CP(2)$ model generates nontopological solitons satisfying a particular set of first-order differential equations.

In order to introduce our results, this manuscript is organized as follows. In Sec. II, we introduce the overall

$CP(N-1)$ model and the definitions inherent to it, from which we verify that $A^0 = 0$ holds as a legitimate gauge choice (and thus the theory engenders configurations with no electric field). Next, for the sake of simplicity, we particularize our study to the $N = 3$ case, while focusing on those static solutions possessing radial symmetry. We then minimize the total energy, from which we find the corresponding first-order equations and the lower bound for the total energy; such a theoretical construction is only possible due to a differential constraint including the dielectric function and the self-interacting potential defining the effective scenario. In Sec. III, we use the first-order differential equations we have found previously to calculate genuine nontopological gauged solitons. The point to be highlighted here is the absence of nontopological profiles for $G(|\phi|) = 1$ (the energy of the resulting structures vanishes identically). We can contour this problem by considering convenient nontrivial forms of the dielectric function. Also, despite the apparent existence of two different solutions, we verify that the effective theory provides a unique phenomenology, at least regarding the nontopological solitons at the classical level. We present the solutions themselves in Sec. IV, and point out the main properties they engender. In Sec. V, we end our manuscript by presenting the final comments and perspectives regarding future contributions.

In what follows, we use $\eta^{\mu\nu} = (+--)$ as the metric signature and the natural units system, for convenience.

II. THE OVERALL MODEL

We begin by presenting the Lagrange density of the gauged $CP(N-1)$ model we consider in this manuscript,

$$\mathcal{L} = -\frac{G(|\phi|)}{4}F_{\mu\nu}F^{\mu\nu} + (P_{ab}D_\mu\phi_b)^* P_{ac}D^\mu\phi_c - V(|\phi|), \tag{1}$$

where greek indices run over time-space coordinates, and latin ones represent the internal indices of the complex $CP(N-1)$ field. Here, $F_{\mu\nu} = \partial_\mu A_\nu - \partial_\nu A_\mu$ is the standard electromagnetic field-strength tensor, with $P_{ab} = \delta_{ab} - h^{-1}\phi_a\phi_b^*$ being a projection operator introduced in a convenient way. Moreover, $D_\mu\phi_a = \partial_\mu\phi_a - igA_\mu Q_{ab}\phi_b$ stands for the covariant derivative, with Q_{ab} being a real and diagonal charge matrix. The function $G(|\phi|)$ multiplying the Maxwell term stands for a dielectric function to be chosen conveniently later below; the resulting model represents an effective action describing a system in a medium defined by such a dielectric function. The $CP(N-1)$ field ϕ itself is constrained to satisfy $\phi_a^*\phi_a = h$.

The static Gauss' law inherent to the model (1) reads

$$\partial_j(G\partial^j A^0) = J^0, \tag{2}$$

(with j running over spatial coordinates only) with J^0, the charge density, given by

$$J^0 = ig[(P_{ab}D^0\phi_b)^* P_{ac}Q_{cd}\phi_d - P_{ab}D^0\phi_b(P_{ac}Q_{cd}\phi_d)^*], \tag{3}$$

where $D^0\phi_b = -igQ_{bc}\phi_c A^0$. It is evident that the gauge $A^0 = 0$ satisfies Eq. (2) identically. Therefore, it is possible to infer that the resulting time-independent solutions do not exhibit an electric field.

In what follows, we particularize our investigation to the case of the gauged $CP(2)$ model, for the sake of simplicity. Then, we focus our attention on those time-independent radially symmetric configurations defined by the following ansatz:

$$A_i = -\frac{1}{gr}\epsilon^{ij}n^j A(r), \tag{4}$$

$$\begin{pmatrix}\phi_1\\ \phi_2\\ \phi_3\end{pmatrix} = h^{\frac{1}{2}}\begin{pmatrix}e^{im_1\theta}\sin(\alpha(r))\cos(\beta(r))\\ e^{im_2\theta}\sin(\alpha(r))\sin(\beta(r))\\ e^{im_3\theta}\cos(\alpha(r))\end{pmatrix}, \tag{5}$$

where m_1, m_2, and $m_3 \in \mathbb{Z}$ are winding numbers, ϵ^{ij} stands for the bidimensional Levi-Civita symbol (with $\epsilon^{12} = +1$), and $n^j = (\cos\theta, \sin\theta)$ is the position unit vector.

In such a context, regular configurations possessing no divergences are attained via those profile functions $\alpha(r)$ and $A(r)$ fulfilling

$$\alpha(r\to 0)\to 0 \quad \text{and} \quad A(r\to 0)\to 0. \tag{6}$$

Moreover, given that we are interested in nontopological solitons, the profile functions $\alpha(r)$ and $A(r)$ must satisfy

$$\alpha(r\to\infty)\to 0 \quad \text{and} \quad A'(r\to\infty)\to 0, \tag{7}$$

with $A(r\to\infty)\equiv A_\infty$ finite and arbitrary.

At this point, it is important to clarify that, regarding the charge matrix Q_{ab} and the winding numbers m_1, m_2, and m_3, there are two different combinations supporting first-order solutions: (i) $Q = \lambda_3/2$ and $m_1 = -m_2 = m$, and (ii) $Q = \lambda_8/2$ and $m_1 = m_2 = m$ [both with $m_3 = 0$, and λ_3 and λ_8 standing for the diagonal Gell-Mann matrices: $\lambda_3 = \mathrm{diag}(1,-1,0)$ and $\sqrt{3}\lambda_8 = \mathrm{diag}(1,1,-2)$]. However, it is known that these two combinations are phenomenologically equivalent since they simply mimic each other, and therefore only one effective scenario exists, as demonstrated in Ref. [9]. Hence, in this work, we consider only the first choice (i.e., $m_1 = -m_2 = m$, $m_3 = 0$, and $Q = \lambda_3/2$), for convenience.

The second-order Euler-Lagrange equation for the additional profile function $\beta(r)$ is

$$\frac{d^2\beta}{dr^2}+\left(\frac{1}{r}+2\frac{d\alpha}{dr}\cot\alpha\right)\frac{d\beta}{dr}=\frac{\sin^2\alpha\sin(4\beta)}{r^2}\left(m-\frac{A}{2}\right)^2. \tag{8}$$

We are interested in solutions where β is a constant; such solutions are ($k\in Z$)

$$\beta(r)=\beta_1=\frac{\pi}{4}+\frac{\pi}{2}k \quad \text{or} \quad \beta(r)=\beta_2=\frac{\pi}{2}k, \tag{9}$$

which apparently splits our investigation into two distinct branches. However, it is important to say that, when considering topological first-order solitons, these two branches engender the very same phenomenology, and are thus physically equivalent. Below, we demonstrate that such an equivalence also holds regarding nontopological solitons.

We now look for first-order differential equations providing genuine solutions of the model (1) by minimizing its total energy. In this case, given the radially symmetric ansatz (4) and (5), the effective energy reads

$$\frac{E}{2\pi}=\int\left(\frac{1}{2}GB^2+V\right)rdr + h\int\left[\left(\frac{d\alpha}{dr}\right)^2+\frac{W}{r^2}\left(\frac{A}{2}-m\right)^2\sin^2\alpha\right]rdr, \tag{10}$$

with $W=W(\alpha,\beta)=1-\sin^2\alpha\cos^2(2\beta)$, where the function $\beta(r)$ is necessarily one of those presented in Eq. (9), and $B(r)=-A'/gr$ stands for the magnetic field (here, a prime denotes a derivative with respect to the radial coordinate r). We then write the expression (10) in the form

$$\frac{E}{2\pi}=\int\left[\frac{G}{2}\left(B\mp\sqrt{\frac{2V}{G}}\right)^2\pm B\sqrt{2GV}\right]rdr + h\int\left[\frac{d\alpha}{dr}\mp\frac{\sqrt{W}}{r}\left(\frac{A}{2}-m\right)\sin\alpha\right]^2rdr \mp\int\left[\frac{d(A-2m)}{dr}\frac{\sqrt{2GV}}{g}+(A-2m)h\sqrt{W}\frac{d\cos\alpha}{dr}\right]dr. \tag{11}$$

In what follows, we impose the constraint

$$\frac{d}{dr}(\sqrt{2GV})=gh\sqrt{W}\frac{d}{dr}\cos\alpha, \tag{12}$$

via which we rewrite Eq. (11) as

$$E=E_{bps}+\pi\int G\left(B\mp\sqrt{\frac{2V}{G}}\right)^2rdr + 2\pi h\int\left[\frac{d\alpha}{dr}\mp\frac{\sqrt{W}}{r}\left(\frac{A}{2}-m\right)\sin\alpha\right]^2rdr, \tag{13}$$

with the energy bound E_{bps} given by

$$E_{bps}=2\pi\int r\varepsilon_{bps}dr, \tag{14}$$

where

$$\varepsilon_{bps}=\mp\frac{2}{gr}\frac{d}{dr}\left[\left(\frac{A}{2}-m\right)\sqrt{2GV}\right], \tag{15}$$

with the upper (lower) sign holding for negative (positive) values of m. In this case, the lower bound (14) can be easily calculated, i.e.,

$$E_{bps}=\mp\frac{2\pi}{g}[(A_\infty-2m)\sqrt{2G_\infty V_\infty}+2m\sqrt{2G_0V_0}], \tag{16}$$

where $G_0\equiv G(r\to 0)$, $V_0\equiv V(r\to 0)$, $G_\infty\equiv G(r\to\infty)$, and $V_\infty\equiv V(r\to\infty)$, with G_0V_0 and $G_\infty V_\infty$ non-negative and finite.

Now, given the expression (13), one concludes that the field solutions saturating the energy lower bound (16) are those satisfying

$$B=\pm\sqrt{\frac{2V}{G}}, \tag{17}$$

and

$$\frac{d\alpha}{dr}=\pm\frac{\sin\alpha}{r}\left(\frac{A}{2}-m\right)\sqrt{1-\sin^2\alpha\cos^2(2\beta)}, \tag{18}$$

which stand for the first-order equations related to the effective radially symmetric scenario. Here, it is important to highlight that the self-duality supporting the first-order equations (17) and (18) holds only in the presence of the constraint (12), as such a constraint allows us to rewrite the energy (10) in the form (13) via the Bogomol'nyi prescription [2].

It is also interesting to calculate the magnetic flux Φ_B that the radially symmetric configurations support. It reads

$$\Phi_B=2\pi\int rB(r)dr=-\frac{2\pi}{g}A_\infty, \tag{19}$$

with $A_\infty\equiv A(r\to\infty)$ being not necessarily proportional to the winding number m, as both the magnetic flux and the energy lower bound (16) are not quantized.

In the next section, we show how the first-order expressions we have introduced above can be used to generate well-behaved nontopological structures possessing finite energy; these configurations satisfy the radially symmetric Euler-Lagrange equations, and thus represent legitimate solutions of the corresponding model. In this manuscript, for simplicity, we consider those cases fulfilling $G_0V_0=G_\infty V_\infty$, where the energy of the resulting configurations is

$$E = E_{bps} = \mp \frac{2\pi}{g} A_\infty \sqrt{2G_\infty V_\infty}, \tag{20}$$

with $G_\infty V_\infty$ being positive and finite.

III. NONTOPOLOGICAL FIRST-ORDER SCENARIOS

We now go further in our investigation by using the first-order framework we have introduced previously to obtain finite-energy nontopological solitons. We proceed according the following prescription. First, we pick a particular solution for the function $\beta(r)$ coming from Eq. (9), from which we solve the differential constraint (12) in order to get a concrete relation between the dielectric function $G(|\phi|)$ and the self-interacting potential $V(|\phi|)$. We then choose $G(|\phi|)$ conveniently, and thus get the potential $V(|\phi|)$ defining that particular model, and also write down the corresponding first-order equations (17) and (18). We particularize the expression for the radially symmetric energy density coming from Eq. (10), with the functions $\alpha(r)$ and $A(r)$ obeying the asymptotic boundary conditions (7). Finally, we use such conditions together with those in Eq. (6) in order to solve the first-order differential equations numerically, from which we depict the resulting profiles for $\alpha(r)$, $A(r)$, the magnetic field, and the energy density they engender. We also calculate the corresponding total energy (20) and magnetic flux (19) explicitly.

It is important to discuss the absence of nontopological solitons within the usual model, i.e., for $G(|\phi|) = 1$. In this case, the energy lower bound (20) reduces to $E = E_{bps} = \mp 2\pi g^{-1} A_\infty \sqrt{2V_\infty}$. The point to be raised is that, in order to fulfill the finite-energy requirement $\varepsilon(r \to \infty) \to 0$, the self-interacting potential must satisfy $V_\infty \equiv V(r \to \infty) \to 0$, from which one also gets $E_{bps} = 0$, as the corresponding solutions are energetically irrelevant.

Therefore, in this work, in order to avoid the aforementioned scenario, we consider nontrivial expressions for the dielectric function $G(|\phi|)$.

Next, we study the cases with $\beta(r) = \beta_1$ and $\beta(r) = \beta_2$ separately.

A. The $\beta(r) = \beta_1$ case

It was demonstrated recently [10] that such a case gives rise to well-behaved first-order topological solitons with radial symmetry. Now, we go a little bit further by investigating the nontopological structures $\beta(r) = \beta_1$ supports. In this sense, we choose

$$\beta(r) = \beta_1 = \frac{\pi}{4} + \frac{\pi}{2} k, \tag{21}$$

via which the differential constraint (12) can be reduced to

$$\frac{d}{dr}(\sqrt{2GV}) = \frac{d}{dr}(gh\cos\alpha), \tag{22}$$

and its solution defines the potential $V(\alpha)$ in terms of the dielectric function $G(\alpha)$, i.e.,

$$V(\alpha) = \frac{g^2 h^2}{2G(\alpha)} \cos^2\alpha, \tag{23}$$

where the integration constant was conveniently set to zero.

Here, given the expression (23), one notes that $G = 1$ (the standard case, in the absence of the dielectric function) leads to a self-interacting potential with no symmetric vacuum, therefore giving rise to topological configurations only. In this sense, the dielectric function in Eq. (23) must be chosen in order to engender a potential exhibiting a symmetric vacuum, as such a symmetric point supports the existence of nontopological solitons. We then proceed by fixing

$$G(\alpha) = \frac{(\cos\alpha)^{2-2M}}{1-\cos\alpha}, \tag{24}$$

where $M = 1, 2, 3$ and so on. In this case, we get the potential

$$V(\alpha) = \frac{g^2 h^2}{2} (\cos\alpha)^{2M} (1 - \cos\alpha), \tag{25}$$

which is positive for all values of the parameter M [the resulting energy is itself positive, which justifies the way M enters the definition (24)]. Thus, the general first-order equations (17) and (18) are reduced to

$$\frac{1}{r}\frac{dA}{dr} = \pm\lambda^2 (\cos\alpha)^{2M-1} (\cos\alpha - 1), \tag{26}$$

$$\frac{d\alpha}{dr} = \pm \frac{\sin\alpha}{r} \left(\frac{A}{2} - m \right), \tag{27}$$

respectively, where the parameter λ stands for

$$\lambda = \sqrt{g^2 h}. \tag{28}$$

We summarize the scenario as follows: given the dielectric function (24) and the self-interacting potential (25), the gauged $CP(N-1)$ model (1) (with $N = 3$) supports radially symmetric time-independent solitons of the form (4) and (5) [with $\beta(r)$ as in Eq. (21)] satisfying the first-order equations (26) and (27), while behaving according to the boundary conditions in Eqs. (6) and (7). Here, it is worthwhile to point out that, for fixed values of M and λ, the equations (26) and (27) support well-behaved solutions only for those values of m for which the condition $0 \leq \alpha(r) < \pi/2$ is fulfilled.

The energy density for such nontopological solitons satisfying the first-order differential equations is

$$\varepsilon(r) = g^2h^2(1-\cos\alpha)(\cos\alpha)^{2M} + 2h\frac{\sin^2\alpha}{r^2}\left(\frac{A}{2}-m\right)^2, \tag{29}$$

which is explicitly positive and attains the finite-energy condition $\varepsilon(r\to\infty)\to 0$.

It is interesting to investigate the way the profile functions $\alpha(r)$ and $A(r)$ behave near the boundaries. In this sense, we linearize the first-order equations (26) and (27), from which we calculate the behavior of these functions near the origin, i.e.,

$$\alpha(r) \approx C_m(\lambda r)^m - \frac{C_m^3}{16(m+1)^2}(\lambda r)^{3m+2} + \cdots, \tag{30}$$

$$A(r) \approx \frac{C_m^2}{4(m+1)}(\lambda r)^{2m+2} - \frac{(12M-5)C_m^4}{48(2m+1)}(\lambda r)^{4m+2} + \cdots, \tag{31}$$

where the asymptotic behavior (i.e., for $r\to\infty$) reads

$$\alpha(r) \approx \frac{C}{(\lambda r)^{\delta_m}} + \cdots, \tag{32}$$

$$A(r) \approx 2m + 2\delta_m - \frac{C^2}{4(\delta_m-1)(\lambda r)^{2\delta_m-2}} + \cdots, \tag{33}$$

where we have set $A_\infty \equiv A(r\to\infty) = 2m+2\delta_m$, and C_m, C, and δ_m stand for real and positive constants to be determined numerically by requiring the proper behavior near the origin and asymptotically, respectively.

It is known that the solution $\beta(r)=\beta_2=\pi k/2$ gives rise to first-order topological configurations possessing finite energy. Next, we discuss the way such a solution engenders nontopological solitons as well.

B. The $\beta(r)=\beta_2$ case

We now investigate the first-order nontopological configurations that $\beta(r)=\beta_2$ supports. In this sense, we choose

$$\beta(r) = \beta_2 = \frac{\pi}{2}k, \tag{34}$$

and the constraint (12) can be rewritten in the form

$$\frac{d}{dr}(\sqrt{2GV}) = \frac{d}{dr}\left(\frac{gh}{2}\cos^2\alpha\right), \tag{35}$$

whose solution is

$$V(\alpha) = \frac{g^2h^2}{32G(\alpha)}\cos^2(2\alpha), \tag{36}$$

where the integration constant was chosen to be $-gh/4$. Again, we have found a relation between the dielectric function and the potential defining the model.

We proceed in the very same way as before, i.e., in order to have a potential with a symmetric vacuum [which therefore supports nontopological profiles; see the discussion just before Eq. (24)], we choose the dielectric function as

$$G(\alpha) = \frac{(\cos(2\alpha))^{2-2M}}{1-\cos(2\alpha)}. \tag{37}$$

(As we demonstrate below, the factor 2α was introduced in Eq. (37) in order to make the two *a priori* different scenarios phenomenologically equivalent via a suitable redefinition.) Then, we get

$$V(\alpha) = \frac{g^2h^2}{32}(\cos(2\alpha))^{2M}(1-\cos(2\alpha)), \tag{38}$$

where the potential itself and its energy density are positive for all M, and thus the corresponding first-order equations (17) and (18) are

$$\frac{1}{r}\frac{dA}{dr} = \pm\frac{g^2h}{4}(\cos(2\alpha))^{2M-1}(\cos(2\alpha)-1), \tag{39}$$

$$\frac{d\alpha}{dr} = \pm\frac{\sin(2\alpha)}{2r}\left(\frac{A}{2}-m\right), \tag{40}$$

respectively. In order to obtain nontopological structures, the above first-order equations must be solved according to the boundary conditions (6) and (7), with the energy density of the resulting solutions being

$$\varepsilon(r) = \frac{g^2h^2}{16}(\cos(2\alpha))^{2M}(1-\cos(2\alpha)) + \frac{h}{2}\frac{\sin^2(2\alpha)}{r^2}\left(\frac{A}{2}-m\right)^2. \tag{41}$$

It is known that, regarding the first-order topological configurations, the two *a priori* different scenarios that the solutions for $\beta(r)$ in Eq. (9) engender simply mimic each other, and therefore only one effective case exists. Here, it is important to highlight that such a correspondence also holds regarding the first-order nontopological structures we have introduced above, i.e., both the dielectric function in Eq. (24) and the self-interacting potential in Eq. (25) can be rewritten as those in Eqs. (37) and (38), respectively, depending on whether we implement the redefinitions $\alpha\to 2\alpha$ and $h\to h/4$. The corresponding first-order equations (26) and (27) then reduce to Eqs. (39) and (40); thus, only one effective scenario exists, at least regarding the nontopological radially symmetric first-order solitons in the presence of a nontrivial dielectric function.

Therefore, from now on, we investigate only the case defined by $\beta(r)=\beta_1$, and the resulting first-order equations are Eqs. (26) and (27).

IV. THE SOLUTIONS

It is instructive to point out that the first-order equations (26) and (27) support approximate analytical solutions describing the corresponding nontopological configurations. In what follows, we investigate these solutions by choosing $m>0$ only (i.e., the lower signs in the first-order expressions), for simplicity. We also suppose that $\alpha(r)\ll 1$ for all values of λr. In this sense, the first-order equations (26) and (27) reduce, respectively, to

$$\frac{1}{r}\frac{dA}{dr}=\mp\frac{\lambda^2}{2}\alpha^2, \tag{42}$$

$$\frac{d\alpha}{dr}=\pm\frac{\alpha}{r}\left(\frac{A}{2}-m\right), \tag{43}$$

which can be combined to form the Liouville equation for the profile function $\alpha(r)$, i.e.,

$$\frac{d^2(\ln\alpha^2)}{dr^2}+\frac{1}{r}\frac{d(\ln\alpha^2)}{dr}+\frac{\lambda^2}{2}\alpha^2=0, \tag{44}$$

whose general solution is [13]

$$\alpha(r)=\frac{4C}{\lambda r_0}\frac{(\frac{r}{r_0})^{C-1}}{1+(\frac{r}{r_0})^{2C}}, \tag{45}$$

with C and r_0 standing for integration constants. Here, it is interesting to note that this solution satisfies the conditions $\alpha(r\to 0)\to 0$ and $\alpha(r\to\infty)\to 0$ for $C>1$ only.

In addition, given the solution (45), the first-order equation (43) provides

$$A(r)=2(m+1)-2C+\frac{4C(\frac{r}{r_0})^{2C}}{1+(\frac{r}{r_0})^{2C}}, \tag{46}$$

which fulfills $A(r\to 0)\to 0$ only for $C=m+1$. Therefore, the approximate solutions (45) and (46) can be rewritten, respectively, as

$$\alpha_m(r)=\frac{4(m+1)}{\lambda r_0}\frac{(\frac{r}{r_0})^{m}}{1+(\frac{r}{r_0})^{2m+2}}, \tag{47}$$

$$A_m(r)=4(m+1)\frac{(\frac{r}{r_0})^{2m+2}}{1+(\frac{r}{r_0})^{2m+2}}, \tag{48}$$

from which one also gets approximate expressions for the magnetic field,

$$B_m(r)=-\frac{gh}{2}\alpha_m^2, \tag{49}$$

and the energy density,

$$\varepsilon_{bps,m}(r)=\frac{g^2h}{2}\alpha_m^2+2h\frac{\alpha_m^2}{r^2}\left(\frac{A_m}{2}-m\right)^2, \tag{50}$$

with $\alpha_m(r)$ and $A_m(r)$ being given by Eqs. (47) and (48), respectively. The approximate value for $A_\infty\equiv A(r\to\infty)$ can be calculated exactly, i.e.,

$$A_{\infty,m}\equiv A_m(r\to\infty)=4(m+1). \tag{51}$$

The maximum value of Eq. (47) is given by

$$\alpha_m(r_{\max})=\frac{2(m+2)}{\lambda r_0}\left(\frac{m}{m+2}\right)^{\frac{m}{2(m+1)}}, \tag{52}$$

where

$$r_{\max}=r_0\left(\frac{m}{m+2}\right)^{\frac{1}{2(m+1)}}, \tag{53}$$

which approximates r_0 for large values of m. Our previous assumption $\alpha(r)\ll 1$ holds if the additional condition

$$\lambda r_0\gg 2(m+2)\left(\frac{m}{m+2}\right)^{\frac{m}{2(m+1)}} \tag{54}$$

is fulfilled. Therefore, for fixed values of g, h, and r_0, only some values of the integer winding number m are allowed.

We highlight that, given the dielectric function (24), the self-interacting potential (25), and the boundary value (51), the resulting energy bound (20) can be calculated explicitly (remember that $m>0$):

$$E_{bps}=8\pi(m+1)h, \tag{55}$$

where we have used $G_0V_0=G_\infty V_\infty=g^2h^2/2$ (thus verifying our previous conjecture). The corresponding magnetic flux (19) reads

$$\Phi_B=-\frac{8\pi}{g}(m+1), \tag{56}$$

from which we get that $E_{bps}=-gh\Phi_B$. Thus, the energy of the first-order solitons is proportional to their magnetic flux, as expected.

In what follows, we numerically study the first-order equations (26) and (27) by means of the finite-difference scheme, while using the boundary conditions (6) and (7). We adopt $m>0$ (lower signs) and $M=g=h=1$, for simplicity. In this sense, we plot the numerical solutions to the profile functions $\alpha(r)$ and $A(r)$, the magnetic field $B(r)$,

and the energy density $\varepsilon_{bps}(r)$. In these figures, we use the dimensionless variable λr in order to depict the numerical profiles, and the only remaining free parameter remaining is λr_0.

We begin our analysis by depicting the numerical profiles corresponding to the approximate expressions in Eqs. (47) and (48). We choose $m = 1$, while varying λr_0, as the analytical solutions approximate the numerical ones for large values of such a parameter. Here, the dashed lines represent the numerical solutions, and the dotted lines represent the approximate ones (see Figs. 1–4).

In Fig. 1, we show the solutions to the profile function $\alpha(r)$ for $\lambda r_0 = 15$ (blue lines), $\lambda r_0 = 20$ (red lines), and $\lambda r_0 = 30$ (black lines). We see that the resulting profiles are rings centered at the origin, and their amplitudes (radii) decrease (increase) as λr_0 itself increases. The numerical results fulfill our previous assumption [i.e., that $\alpha(r) \ll 1$ for all λr)], and the approximate solutions fit relatively well.

The solutions to the field $A(r)$ are those shown in Fig. 2, from which we see that these profiles approach the approximate boundary condition $A_m(r \to \infty) = 4(m+1)$ in a monotonic way whenever λr_0 increases. In particular, one gets the numerical values $A_1(r \to \infty) \approx 8.07855$ for $\lambda r_0 = 15$, $A_1(r \to \infty) \approx 8.04565$ for $\lambda r_0 = 20$, and $A_1(r \to \infty) \approx 8.02063$ for $\lambda r_0 = 30$.

In Fig. 3, we depict the numerical solutions to the magnetic field $B(r)$, in units of gh. These profiles behave like those for $\alpha(r)$: their amplitudes (radii) decrease

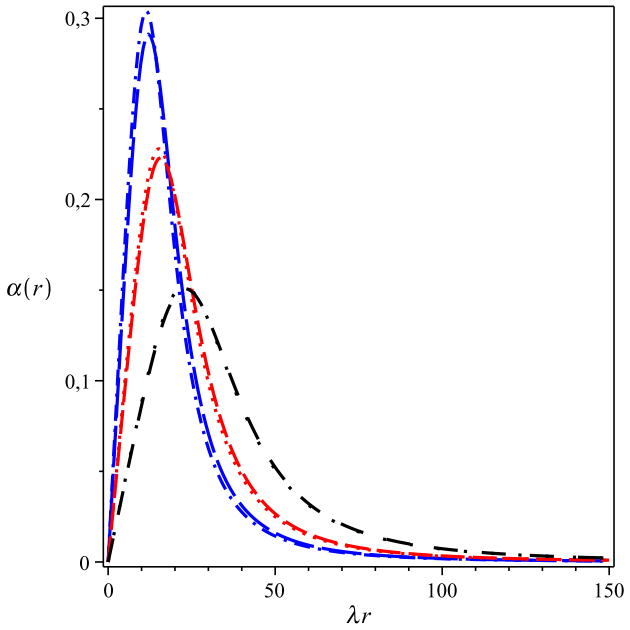

FIG. 1. Solutions to $\alpha(r)$ for $\lambda r_0 = 15$ (blue lines), $\lambda r_0 = 20$ (red lines), and $\lambda r_0 = 30$ (black lines). Here, $M = g = h = m = 1$; the dashed lines stand for the numerical solutions, and the dotted lines stand for the approximate ones coming from Eq. (47). The profiles are rings centered at the origin.

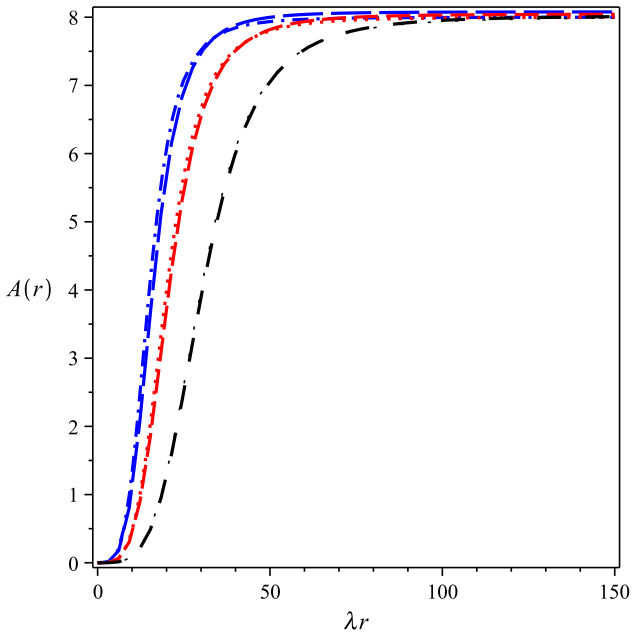

FIG. 2. Solutions to $A(r)$. Conventions are as in the Fig. 1. The approximate results are given by Eq. (48). The numerical solutions approach the approximate value $A_m(r \to \infty) = 4(m+1)$ in a monotonic way whenever λr_0 increases.

(increase) as λr_0 increases. The new solutions also vanish in the asymptotic limit $r \to \infty$, thus fulfilling the finite-energy requirement $\varepsilon(r \to \infty) \to 0$.

The solutions to the energy density $\varepsilon_{bps}(r)$ are shown in Fig. 4, in units of $(gh)^2$, which shows that the

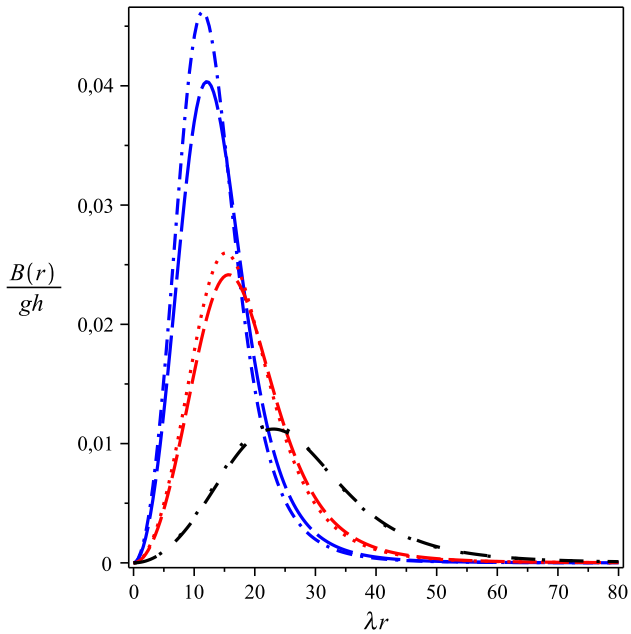

FIG. 3. Solutions to the magnetic field $B(r)$, in units of gh. Conventions are as in the Fig. 1. The approximate solutions come from Eq. (49). Here, the corresponding amplitudes (radii) decrease (increase) as λr_0 itself increases.

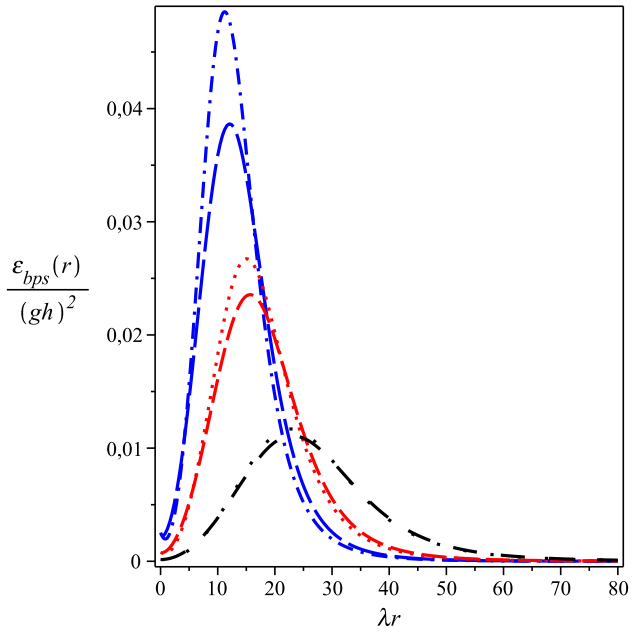

FIG. 4. Solutions to the energy density $\varepsilon_{bps}(r)$, in units of $(gh)^2$. Conventions are as in the Fig. 1. The approximate profiles represent Eq. (50). The nontopological structures are well localized in space.

corresponding nontopological structures are localized in space. Here, we highlight the manner in which $\varepsilon_{bps}(r=0)$ depends on λr_0: the value increases from 0 (zero) as this free parameter decreases.

It is also interesting to point out the existence of another class of numerical solutions that cannot be predicted by an approximate analytical treatment, as the condition $\alpha(r) \ll 1$ for all λr is not satisfied anymore. These new profiles are calculated for finite (but not large) values of the free parameter λr_0, and in this way they differ from the solutions presented above (see Figs. 5–8).

In order to introduce the aforecited profiles, we again solve Eqs. (26) and (27) numerically, for $m > 0$ and $M = g = h = 1$, via the conditions (6) and (7). However, now we choose $\lambda r_0 = 1$, while varying the winding number—$m = 1$ (solid red line), $m = 2$ (dashed black line), and $m = 3$ (dash-dotted green line)—and we plot the corresponding solutions with respect to the dimensionless variable λr.

In this sense, the solutions to $\alpha(r)$ are those depicted in Fig. 5, from which we see that these profiles behave in a similar manner as before, being rings centered at the origin, with both amplitudes and radii increasing as the vorticity increases.

Figure 6 shows the results for the function $A(r)$, where the additional dotted blue line stands for $m = 4$. Here, it is worthwhile to note the appearance of an interesting internal structure for intermediary values of the dimensionless variable λr. It is also interesting to highlight that the new solutions do not fulfill the previous condition (51), with the new values being $A_1(r \to \infty) \approx 9.64900$, $A_2(r \to \infty) \approx 15.01548$, $A_3(r \to \infty) \approx 20.78517$, and $A_5(r \to \infty) \approx 26.98683$.

The numerical profiles for the magnetic field $B(r)$ are plotted in Fig. 7, in units of gh, from which we see that these solutions are drastically different from the ones appearing in Fig. 3: the new configurations are double

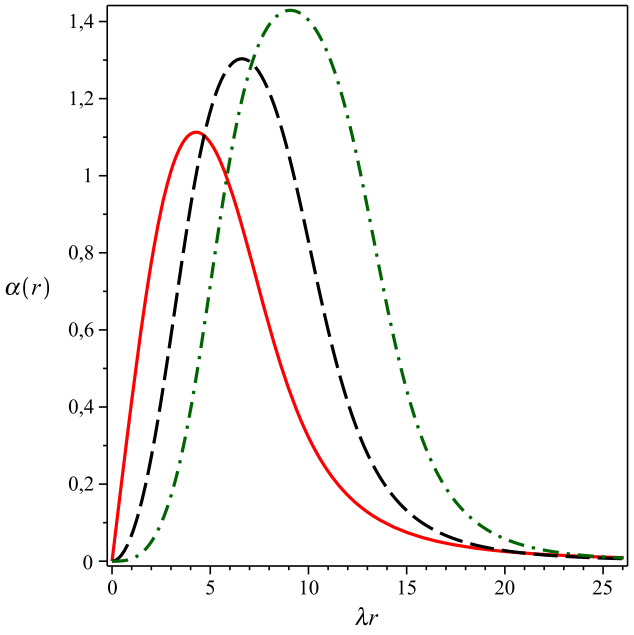

FIG. 5. Solutions to $\alpha(r)$ for $m = 1$ (solid red line), $m = 2$ (dashed black line), and $m = 3$ (dash-dotted green line). Now, $M = g = h = \lambda r_0 = 1$, and the profiles are rings centered at the origin.

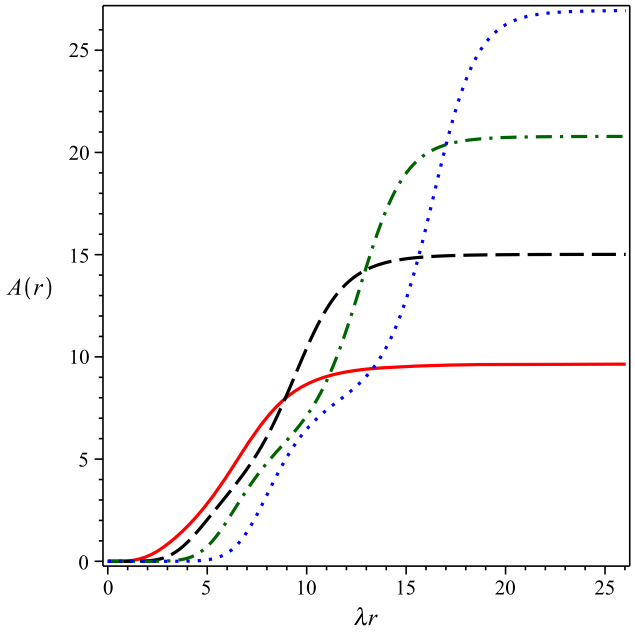

FIG. 6. Solutions to $A(r)$. Conventions are as in the Fig. 5. The additional dotted blue line represents $m = 4$, and the corresponding solution highlights the existence of an internal structure.

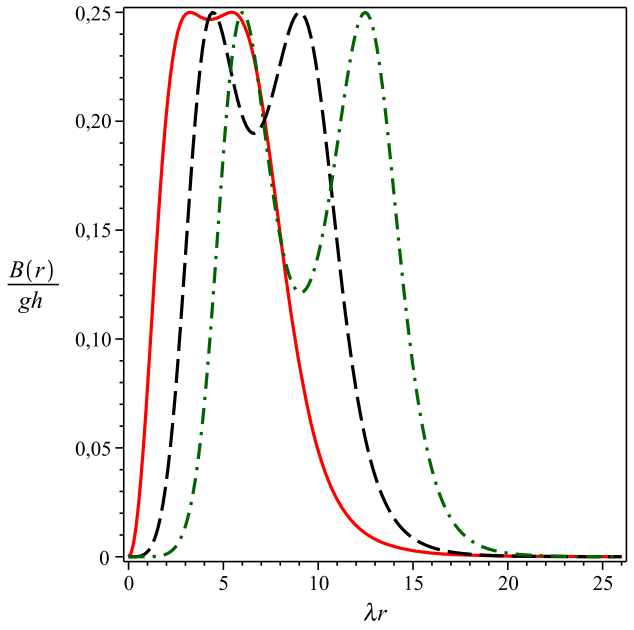

FIG. 7. Solutions to the magnetic field $B(r)$, in units of gh. Conventions are as in the Fig. 5. The new profiles are double rings centered at $r = 0$.

rings centered at $r = 0$, and the magnetic field vanishes in the asymptotic limit.

Finally, Fig. 8 shows the solutions to $\varepsilon_{bps}(r)$, again in units of $(gh)^2$. These profiles also represent double rings centered at the origin. However, in this case, the amplitude of the inner ring is always greater than that of the outer one, and $\varepsilon_{bps}(r = 0)$ vanishes for $m \neq 1$.

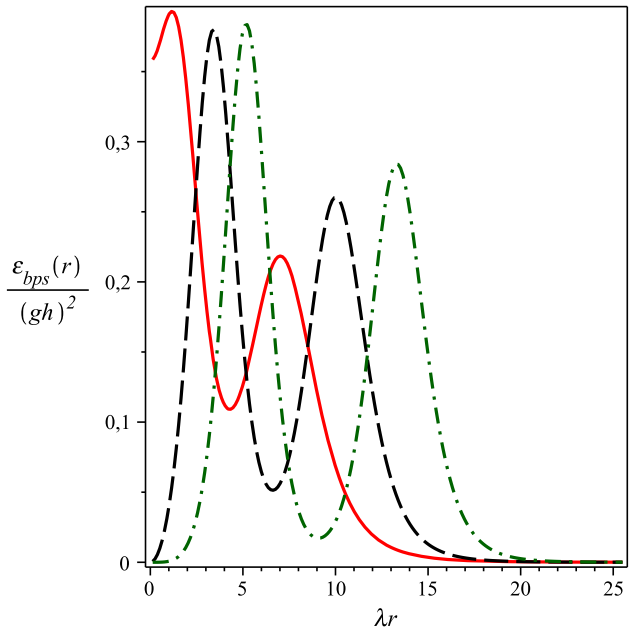

FIG. 8. Solutions to the energy density $\varepsilon_{bps}(r)$, in units of $(gh)^2$. Conventions are as in Fig. 5. Here, $\varepsilon_{bps}(r = 0)$ vanishes for $m \neq 1$.

V. FINAL COMMENTS AND PERSPECTIVES

In this manuscript, we have studied the $CP(2)$ model endowed with the Maxwell term in the presence of an *a priori* arbitrary dielectric function $G(|\phi|)$, from which we have attained nontopological first-order vortices possessing finite energy and nonquantized magnetic flux.

We have presented the particular model and the definitions inherent to it, from which we have verified that $A^0 = 0$ satisfies the static Gauss' law identically, and the resulting time-independent solutions do not support an electric field. We have particularized our investigation to the case $N = 3$, for simplicity. Then, we focused our attention on those radially symmetric configurations described by the ansatz defined in Eqs. (4) and (5) while satisfying the boundary conditions (6) and (7). We introduced convenient choices regarding the charges and winding numbers inherent to the aforementioned ansatz. Then, we calculated the solutions (9) for the additional profile function $\beta(r)$.

We rewrote the expression for the radially symmetric energy (10) as that in Eq. (13), while defining the general first-order equations (17) and (18) satisfied by the fields $\alpha(r)$ and $A(r)$. In addition, we found the corresponding lower bound for the total energy [see Eq. (13) itself and Eq. (20)]. The point to be highlighted here is that such construction was only possible due to the differential constraint (12) including $G(|\phi|)$ and the self-interacting potential $V(|\phi|)$. We also calculated a general result for the magnetic flux Φ_B in Eq. (19).

We discussed the absence of nontopological solitons for $G(|\phi|) = 1$; the energy of these structures vanishes. In order to avoid such a scenario, we considered only nontrivial forms for the dielectric function.

We first studied the case defined by $\beta(r) = \beta_1$ [Eq. (21)], from which we wrote the constraint (12) as in Eq. (22), whose solution is Eq. (23). Then, we chose the dielectric function as shown in Eq. (24), from which we obtained the potential (25) and the first-order equations (26) and (27). We also linearized these equations in order to define the way the nontopological solutions behave near the boundaries.

We also implemented the same prescription for $\beta(r) = \beta_2$ (34), from which we calculated the corresponding first-order expressions. We noticed that the two scenarios defined by the different solutions for $\beta(r)$ can be verified to mimic each other via the redefinitions $\alpha \to 2\alpha$, $\lambda \to \lambda/4$, and $h \to h/4$; therefore, only one effective case exists. In this sense, we only focused our attention on the case $\beta(r) = \beta_1$.

We supposed that $\alpha(r) \ll 1$ for all λr (with $\lambda^2 = g^2 h$), from which we combined the first-order equations (26) and (27); thus, we verified that the function $\alpha(r)$ satisfies the Liouville equation whose analytical solution gives the profiles (47) and (48), and we also calculated the boundary value $A(r \to \infty) \to 4(m + 1)$. In addition, we verified

explicitly that the energy bound is proportional to the magnetic flux inherent to the resulting solitons, and that both quantities are not necessarily quantized, as expected.

We depicted the numerical results we found for $\alpha(r)$, $A(r)$, the magnetic field $B(r)$, and the energy density $\varepsilon_{bps}(r)$, for different values of the vorticity m and the parameter λr_0, from which we pointed out the existence of two different classes of solutions: those coming from large values of λr_0 [which are reasonably well described by the analytic expressions in Eqs. (47) and (48)], and those solutions related to small values of λr_0 (which do not possess an approximate counterpart).

Here, it is important to highlight that the results we have introduced in this work hold only for those time-independent solitons described by the ansatz in Eqs. (4) and (5). In this sense, it is not possible to say that the general model (1) supports regular first-order solutions outside the radially symmetric scenario, as such a question lies beyond the scope of the present investigation.

Moreover, ideas regarding future works include the study of the $CP(2)$ model in the presence of the Chern-Simons action (instead of the Maxwell one) and the first-order configurations the resulting theory possibly supports. This issue is now under consideration, and we hope to report relevant results in a future publication.

ACKNOWLEDGMENTS

The authors thank Coordenação de Aperfeiçoamento de Pessoal de Nível Superior, Conselho Nacional de Desenvolvimento Científico de Tecnológico, and Fundação de Amparo à Pesquisa e ao Desenvolvimento Científico e Tecnológico do Maranhão (Brazilian agencies) for partial financial support.

[1] N. Manton and P. Sutcliffe, *Topological Solitons* (Cambridge University Press, Cambridge, England, 2004).
[2] E. Bogomol'nyi, Sov. J. Nucl. Phys. **24**, 449 (1976); M. Prasad and C. Sommerfield, Phys. Rev. Lett. **35**, 760 (1975).
[3] H. B. Nielsen and P. Olesen, Nucl. Phys. **B61**, 45 (1973).
[4] R. Jackiw and E. J. Weinberg, Phys. Rev. Lett. **64**, 2234 (1990); R. Jackiw, K. Lee, and E. J. Weinberg, Phys. Rev. D **42**, 3488 (1990).
[5] D. Bazeia, E. da Hora, C. dos Santos, and R. Menezes, Phys. Rev. D **81**, 125014 (2010); Eur. Phys. J. C **71**, 1833 (2011); D. Bazeia, R. Casana, M. M. Ferreira, Jr., and E. da Hora, Europhys. Lett. **109**, 21001 (2015); R. Casana, E. da Hora, D. Rubiera-Garcia, and C. dos Santos, Eur. Phys. J. C **75**, 380 (2015); R. Casana and L. Sourrouille, Mod. Phys. Lett. A **29**, 1450124 (2014); L. Sourrouille, Phys. Rev. D **87**, 067701 (2013).
[6] R. Casana, M. M. Ferreira, Jr., E. da Hora, and C. Miller, Phys. Lett. B **718**, 620 (2012); R. Casana, M. M. Ferreira, Jr., E. da Hora, and A. B. F. Neves, Eur. Phys. J. C **74**, 3064 (2014); R. Casana and G. Lazar, Phys. Rev. D **90**, 065007 (2014); R. Casana, C. F. Farias, and M. M. Ferreira, Jr., Phys. Rev. D **92**, 125024 (2015); R. Casana, C. F. Farias, M. M. Ferreira, Jr., and G. Lazar, Phys. Rev. D **94**, 065036 (2016).
[7] C. Armendariz-Picon, T. Damour, and V. Mukhanov, Phys. Lett. B **458**, 209 (1999); V. Mukhanov and A. Vikman, J. Cosmol. Astropart. Phys. 02 (2005) 004; A. Sen, J. High Energy Phys. 07 (2002) 065; C. Armendariz-Picon and E. A. Lim, J. Cosmol. Astropart. Phys. 08 (2005) 007; J. Garriga and V. Mukhanov, Phys. Lett. B **458**, 219 (1999); R. J. Scherrer, Phys. Rev. Lett. **93**, 011301 (2004); A. D. Rendall, Classical Quantum Gravity **23**, 1557 (2006).
[8] A. D'Adda, M. Luscher, and P. D. Vecchia, Nucl. Phys. **B146**, 63 (1978); E. Witten, Nucl. Phys. **B149**, 285 (1979); A. M. Polyakov, Phys. Lett. B **59**, 79 (1975); M. Shifman and A. Yung, Rev. Mod. Phys. **79**, 1139 (2007).
[9] A. Yu Loginov, Phys. Rev. D **93**, 065009 (2016).
[10] R. Casana, M. L. Dias, and E. da Hora, Phys. Lett. B **768**, 254 (2017).
[11] C. M. Hull, A. Karlhede, U. Lindström, and M. Roček, Nucl. Phys. **B266**, 1 (1986).
[12] R. Friedberg and T. D. Lee, Phys. Rev. D **15**, 1694 (1977); **16**, 1096 (1977); **18**, 2623 (1978).
[13] R. Jackiw, K.-M. Lee, and E. J. Weinberg, Phys. Rev. D **42**, 3488 (1990).